ELASTIC BUCKLING OF VERTICAL CANTILEVERED CYLINDERS

JAN BŁACHUT

The University of Liverpool, Mechanical Engineering, Liverpool, U.K.

e-mail: em20@liverpool.ac.uk

The paper details numerical and experimental study on elastic buckling of cylindrical shells caused by external pressure, a horizontal edge force and combined action of both. The following three geometries of vertical cylinders are considered: (i) circular cylinders, (ii) concentric circular cylinders, and (iii) cylinders with elliptical cross-section. In total, test results on nineteen shells are given. The experimental data is benchmarked against the FE predictions of buckling loads. Good agreement has been obtained between the experimental results and numerical predictions for all tested shells except for buckling of the concentric cylinders loaded by the horizontal edge force. Possible reasons for discrepancies are discussed.

The paper offers insight into buckling performance of vertical cylinders subjected to combined loading, and in the case of concentric cylinders, into the interaction between the inner and outer shells. Some of the interaction features, not immediately obvious, are discussed.

Key words: combined stability, shear load, external pressure, concentric cylinders, elliptic cylinders

1. Introduction

Study of vertical cylinders under horizontal edge shear and pressure loading is of relevance to storage tanks and containers, e.g., in nuclear and chemical industries. During earthquakes, vertical cylinders are subjected to horizontal ground acceleration, and the edge shear force represents quasi-static component of earthquake loading. This, in turn, can cause buckling of vertical cylinders. Hence for their safe design, it is essential to properly understand buckling behaviour of cylinders due to external pressure and edge shear loads. There are a few studies on buckling of cylinders under edge shear loads.

A membrane solution for elastic buckling under edge shear load was derived by Lu (1965), Schroeder (1972). However, the most notable study on elastic buckling under the edge shear force is due to Yamaki (1984). A number of tests on cylinders made of polyester films were conducted, and good comparison between experimental results and the analytical solutions was obtained. In addition, tests under combined loading of external pressure and edge shear load were performed on small laboratory scale cylindrical models. These results gave favourable comparison with analytical results on elastic buckling. Welded steel cylinders under the edge shear force were tested by Galletly and Błachut (1985). Those results, as yet, have not been verified by analytical or numerical solutions. Some recent studies on elastic-plastic buckling of vertical, cantilevered steel shells can be found in papers by Gettel and Schneider (2007), and by Athiannan and Palaninathan (2004). The latter paper reviews other known publications on this topic. Thus, it turns out that there are some studies on elastic buckling of cylinders under edge shear and results available on plastic buckling of cylinders are relatively scarce. Another point to be noted is that, in industry, concentric cylinders are being widely used. Study on the behaviour of concentric cylinders under edge load will form a useful extension of the current state of knowledge in this area. Results on the behaviour of concentric cylinders under edge shear are conspicuously absent in the open literature. Similarly, there are no studies on analysis of cylinders with elliptical cross-section under the edge shear force. In the literature, these cylinders are usually termed as elliptic cylinders. However, there are few studies on behaviour of elliptic cylinders under external pressure only. Experimental and analytical study on buckling of elliptic cylinders under external pressure was carried out by Yao and Jenkins (1970). Comparison of experimental buckling results, carried out by Yao and Jenkins (1970), with numerical predictions was published by Bushnell (1971). Marlowe and Brogan (1971) used a nonlinear finite difference program, STAGS to verify some of the results given by Yao and Jenkins (1970). Singer *et al.* (2002) provided a comprehensive review of experimental techniques and results on buckling of cylindrical shells and tubes for a wide rage of loading scenarios. Finally, it is worth mentioning the recent review papers by Öry *et al.* (1998), Rotter (1998), and Błachut and Magnucki (2008). All three papers address other issues encountered in buckling of aerospace shells, pressure vessels, vertical and horizontal storage vessels and silos.

In the present study, the following three types of cylinders are considered: (i) single cylinder with circular cross-section, (ii) two concentric cylinders of circular cross-section, and (iii) single cylinder of elliptical cross-section. First numerical results are obtained with the help of the Finite Elements for a wide

range of geometrical parameters. Then selected configurations are chosen for experimental tests followed by the FE benchmarking.

2.   Numerical results

2.1.   Background and modelling details

When a vertical cantilevered shell is subjected to a horizontal force applied to its top end, one can expect at least one of the following two modes of buckling failure: (i) an axisymmetric bulge occurring over the part of the circumference near the base of the shell (frequently called as "elephant foot's buckling"), and (ii) development of shear lobes – as illustrated in Fig. 1.

(a) Pre-buckling shape   (b) Buckling shape   (c)
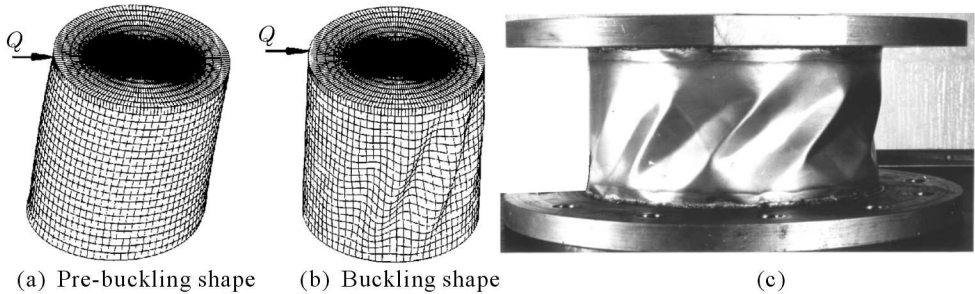
Fig. 1. Shape just prior to buckling (a) and eigenshape (b); collapsed steel
cantilevered shell (c) – all not to scale

Consider a vertical cylinder loaded at its tip by a horizontal force Q. Figure 1a shows the pre-buckling shape of the cylinder just prior to buckling, and Fig. 1b depicts the corresponding eigenshape. This failure form can be elastic or elastic-plastic. The latter is illustrated in Fig. 1c for a steel shell. In the current paper, only elastic shear buckling is considered with the failure modes illustrated in Figs. 1a and 1b. It is assumed that all cylinders are made of Mylar. Elastic properties of the Mylar material are taken as: $E = 5028.5\,\text{MPa}$, $\nu = 0.3$. Thickness of the Mylar sheet is assumed as $0.25\,\text{mm}$ in all the cases. Geometry of various cylinders analysed is shown in Figs, 2a, 2b, and 2c. The cylinders are fixed at the base. At the top, a thick aluminium flange is considered. The FE software ABAQUS (Hibbitt *et al.*, 2004) is used in all FE calculations. Shells are modelled using S8R5 8-noded doubly curved shell elements. The aluminium flange, which is attached at the top of the cylinder, is modelled using C3D8, 8-noded solid elements. The edge shear force Q is

applied at the top edge of the cylinder and it always acts horizontally. The
external pressure P is considered to be uniform and of follower nature.
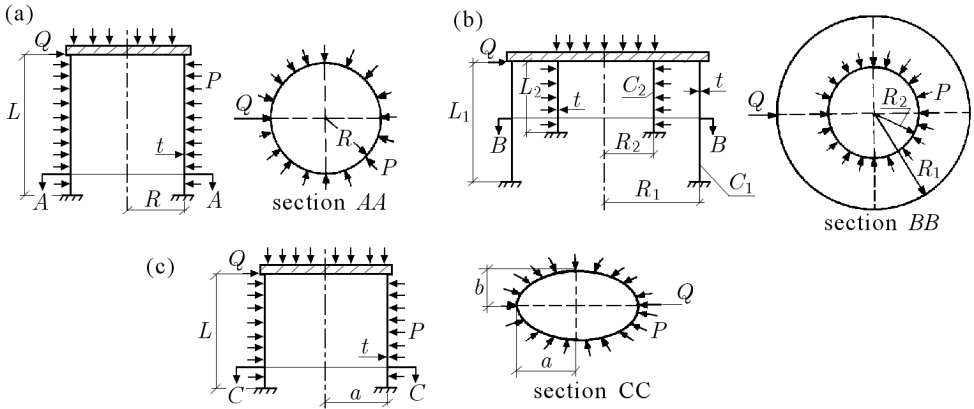
Fig. 2. Geometry of various cylinders: circular cylinder (a); concentric cylinders (b);
elliptic cylinder (c)

2.2. Circular cylinder subjected to edge shear force and external pressure

The first set of calculations was carried out for circular cylinders under a
combined external pressure and an edge shear force. For this purpose, at a
given external pressure, the edge shear force was applied, and the force at
which buckling occurred was taken as the buckling shear force Q_{bif}. This is
done for various values of the external pressure. Buckling modes corresponding
to four different values of the external pressure are shown in Fig. 3. It is seen
that under pure pressure, the buckling mode has a uniform distribution of
circumferential waves, and as the pressure decreases, the torsional effect due
to the edge shear force gets reflected in the buckling mode. The effect of
external pressure on the load-deflection curve under the edge shear force is
shown in Fig. 4a. It is seen that application of the external pressure does not
change the slope of the load-deflection curve. Variation of the buckling edge
shear force with the external pressure is depicted in Fig. 4b. In this figure,
typical domains of combined stability are shown for two values of cylinder's
radius R, i.e., $R = 50\,\text{mm}$ and $100\,\text{mm}$.

2.3. Concentric cylinders subjected to edge shear load and external pressure

Geometry of concentric cylinders is shown in Fig. 2b. The outer cylinder is
denoted as C_1, and the inner cylinder as C_2. Let this system of concentric
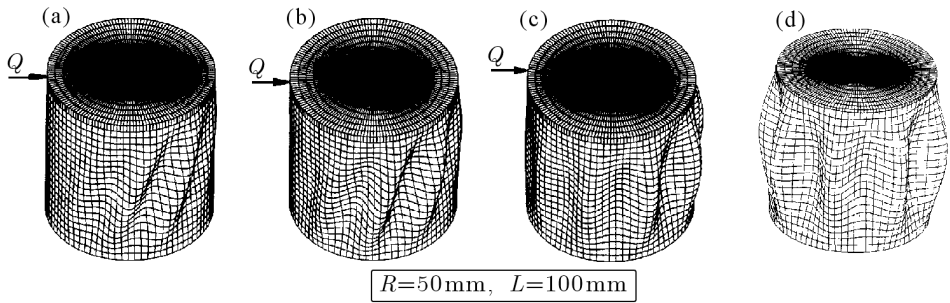
Fig. 3. Buckling modes of circular cylinder under various combinations of the edge shear force and external pressure; (a) $p = 0.0$ MPa, $Q_{bif} = 162.4$ N; (b) $p = 0.003$ MPa, $Q_{bif} = 117.2$ N; (c) $p = 0.0055$ MPa, $Q_{bif} = 40$ N; (d) $p = 0.0059$ MPa (pure pressure)
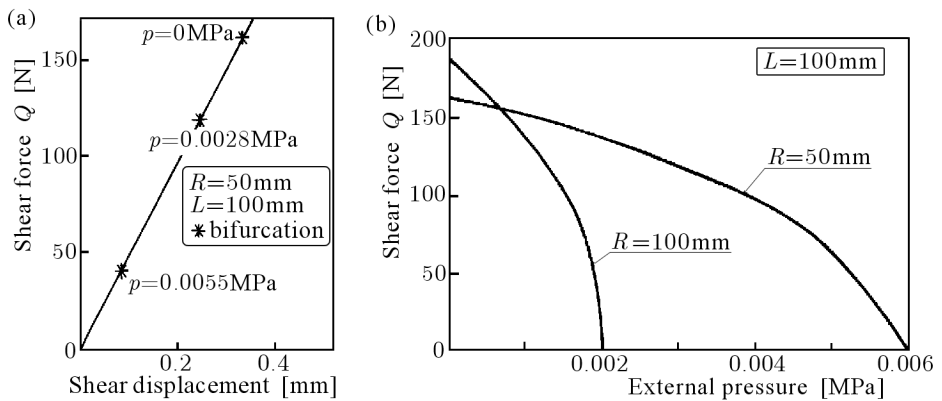
Fig. 4. Effect of the external pressure on the buckling shear force Q_{bif}, and on the load-deflection curve (a). Domains of combined stability for $L/R = 1.0$ and 2.0 (b)

cylinders be initially subjected to the edge shear force only. The load deflection curve for $L_1 = L_2 = 100$ mm, $R_1 = 100$ mm, $R_2 = 50$ mm is shown in Fig. 5. This load-deflection curve is identified as $C_1 + C_2$. Also shown in this figure are load deflection curves of the two cylinders when analysed individually under the edge shear force. These lines are denoted as C_1 and C_2. It is seen that combined cylinders (i.e., concentric cylinders) buckle at a much higher load, and that the critical shear displacement at which buckling occurs is the same as the one corresponding to the outer cylinder. Also, from the buckling mode shown in Fig. 6, it is seen that buckling occurs only in the outer cylinder, and the inner cylinder remains unaffected. In this buckling mode, to show the inner cylinder, some elements of outer cylinders were removed. This was done only for plotting the buckling mode, whilst in the analysis the full cylinder
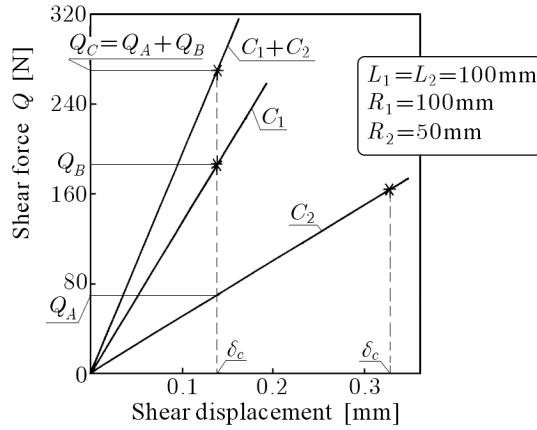
Fig. 5. Load-deflection curve for concentric cylinders under the edge shear force only. Load-deflection curves of inner and outer cylinders when analysed individually are also shown
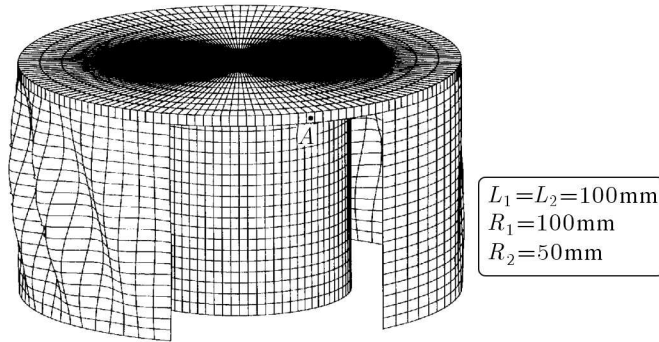
Fig. 6. Buckling mode of concentric cylinders under the edge shear force. Note: the edge shear force is applied at point A

was considered. Another point to be noted in Fig. 5 is that the buckling load corresponding to concentric cylinders is the sum of loads corresponding to the critical displacement δ_c, on the load-deflection curve of two cylinders, when analysed individually. From these observations, one finds that the presence of inner cylinder increases the buckling strength. It should also be noted that δ_c corresponding to the outer cylinder is smaller than the one corresponding to the inner cylinder. Also, buckling of concentric cylinders takes place at δ_c corresponding to the outer cylinder. Thus it is found that the critical shear displacement δ_c plays an important role in buckling of concentric cylinders. In the current case, this implies that at the buckling force, some strength of the inner cylinder was left under-utilised. To make the use of the available

buckling capacity of both cylinders, it is required to have the same δ_c for both cylinders. It is known from previous analyses that δ_c reduces with a decrease in length of the cylinder, see Błachut and Jaiswal (2008). Hence to reduce δ_c corresponding to the inner cylinder its length needs to be decreased. The effect of length of the inner cylinder on the buckling force is shown in Fig. 7. From this figure, it is seen that the magnitude of the buckling shear force becomes smaller with the increase of length of the inner cylinder L_1. However, at one point there is a change in slope of the curve. To the left of this point, buckling occurs in the inner cylinder and to the right of this point, the buckling occurs in outer cylinder. This is illustrated by showing the buckling modes at points a and b in Fig. 7. The eigenshape at a is depicted in Fig. 8a (buckling of the outer cylinder), and the eigenshape at b is shown in Fig. 8b (buckling of the inner cylinder). When δ_c of the inner cylinder is higher than δ_c of the outer one, the buckling occurs in the outer cylinder.
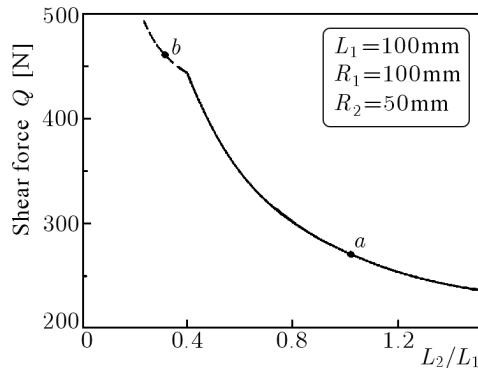
Fig. 7. Effect of length L_2 of the inner cylinder on the buckling shear force of concentric cylinders; - - - buckling of inner cylinder, —— buckling of outer cylinder
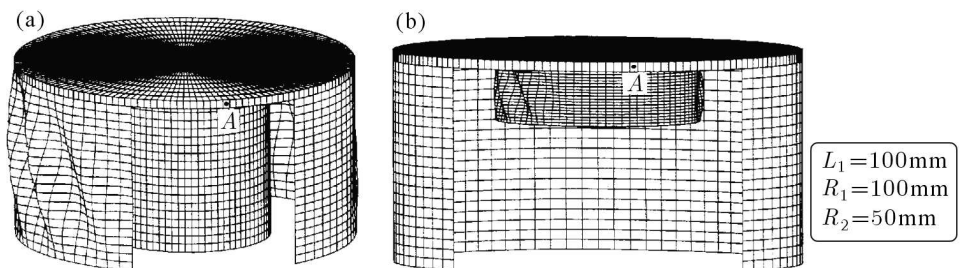
Fig. 8. Buckling modes of concentric cylinders for two different lengths of the inner cylinder. Note: for $L_2 = 100$ mm, buckling occurs in the outer cylinder (a); for $L_2 = 30$ mm, buckling occurs in the inner cylinder (b). The edge shear force is applied at point A

Another way of reducing δ_c of the inner cylinder is to apply external pressure to it. The effect of external pressure on the buckling force of concentric cylinders is shown in Fig. 9. Here the results are presented for three different values of length of the inner cylinder, i.e., $L_2 = 50\,\mathrm{mm}$, $100\,\mathrm{mm}$, and $150\,\mathrm{mm}$. For all the three cases, the results are qualitatively the same, i.e., up to a certain value of pressure, there is no effect on the buckling force and beyond this pressure, buckling force decreases rapidly. For $L_2 = 100\,\mathrm{mm}$, the external pressure does not have any influence on the buckling load up to $0.005\,\mathrm{MPa}$. To understand this behaviour, it is necessary to notice that when the pressure is applied to the inner cylinder, the value of the critical shear displacement δ_c reduces without affecting the slope of the load-deflection curve, Fig. 4a. Thus, the application to pressure on the inner cylinder does not have any influence on buckling of the combined cylinder, so long as the value of δ_c corresponding to the inner cylinder is higher than the one corresponding to the outer cylinder. With the increase of external pressure δ_c corresponding to the inner cylinder becomes equal to that of the outer cylinder. For any further increase in pressure, the failure of combined cylinder occurs due to buckling of the inner cylinder. Hence, further increase in pressure reduces the buckling shear force. To demonstrate this point, the buckling modes corresponding to points a and b in Fig. 9 are shown in Fig. 10.
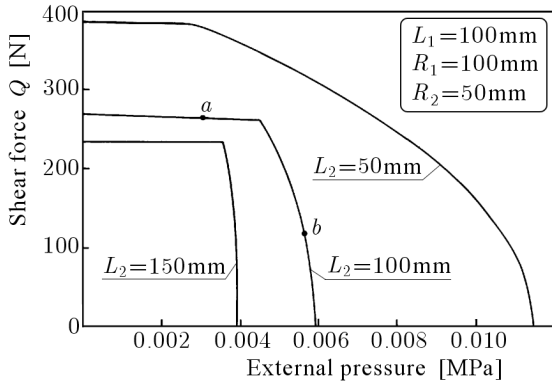
Fig. 9. Domains of combined stability for concentric cylinders. Note: external pressure is only applied to the inner cylinder

2.4. Elliptic cylinders subjected to edge shear force and external pressure

Geometry of an elliptic cylinder is shown in Fig. 2c. First, behaviour of elliptic cylinders under the edge shear force is studied. The dge shear force is applied along the major and the minor axis as well. Buckling modes corresponding to
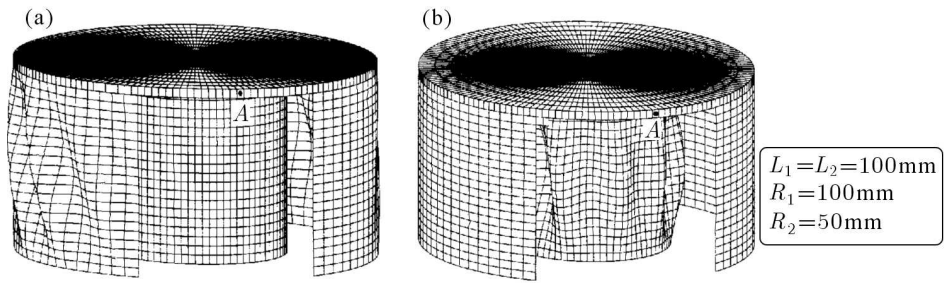
Fig. 10. Effect of external pressure on the buckling mode of concentric cylinders;
(a) $p = 0.003$ MPa and $Q_{bif} = 264.0$ N (buckling occurs in the outer cylinder);
(b) $p = 0.0055$ MPa and $Q_{bif} = 143.9$ N (buckling occurs in the inner cylinder)
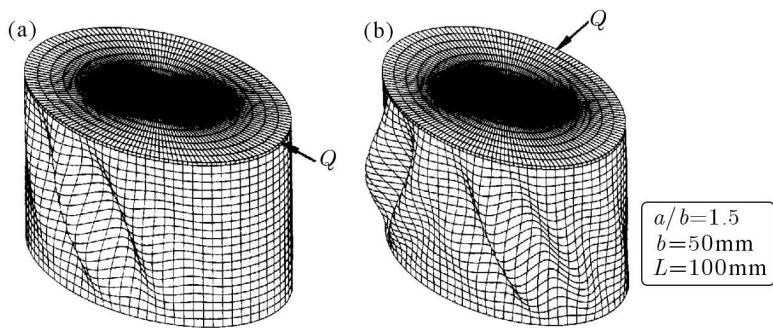
Fig. 11. Buckling modes of an elliptic cylinder under the edge shear force applied
along the major axis (a), and applied along the minor axis (b)
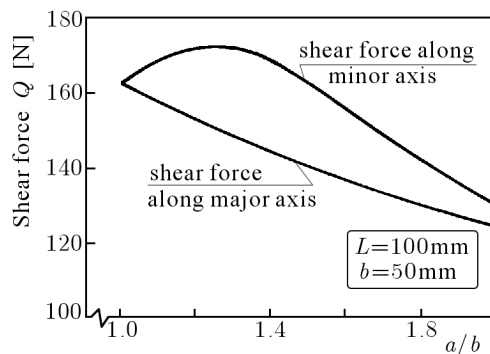
Fig. 12. Effect of the semi-axes ratio a/b on the buckling shear force of the elliptic
cylinder

both cases are illustrated in Fig. 11 for $a/b = 1.5$, $b = 50$ mm and $L = 100$ mm. Next, the effect of semi-axes ratio a/b on the buckling shear force and buckling pressure is studied. Length of the minor axis $2b$ is kept constant and length of the major axis $2a$ is varied. Effect of the (a/b)-ratio on the buckling shear force is shown in Fig. 12. Results are shown for the shear force along the major axis and also along the minor axis.

Next, buckling of elliptic cylinders under external pressure was studied. It was found that under external pressure, elliptic cylinders fail by buckling bifurcation. For $a/b = 1.5$, $b = 50$ mm and $L = 100$ m, the buckling mode under external pressure is shown in Fig. 13. Effect of a/b ratio on buckling pressure is shown in Fig. 14a. In all the cases considered here, the cylinders failed by buckling bifurcation. It is worth mentioning that earlier Bushnell (1971), and Marlowe and Brogan (1971), obtained numerical solutions for elliptic cylinders under external pressure. Various cases considered by them were the ones corresponding to experiments by Yao and Jenkins (1970). In those cases, elliptic cylinders failed by snap-through buckling or collapse. These tests were done on thick elliptic cylinders with the maximum value of $b/t = 68.96$. In the present study, elliptic cylinders considered are thin ones with $b/t = 200.0$, and hence failure is due to buckling bifurcation. For some cases of Yao and Jenkins (1970), numerical calculations were performed using ABAQUS, and the results are shown in the last column of Table 1.

$a/b=1.5$
$b=50$mm
$L=100$mm
$P_{bif}=0.00146$ MPa
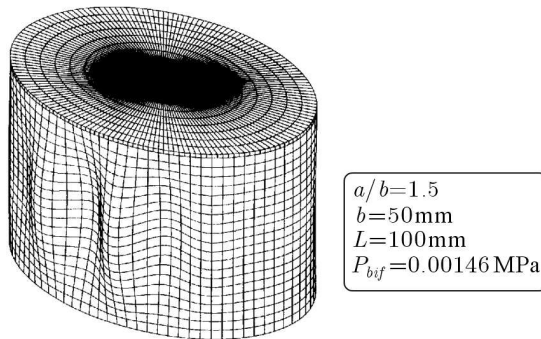
Fig. 13. Buckling mode of an elliptic cylinder under external pressure

The next set of calculations was carried out for elliptic cylinders under a combined edge shear force and external pressure loading. The results showing the effect of external pressure on the buckling shear force are depicted in Fig. 14b. These results are for $L = 100$ mm, $a/b = 1.5$, and $b = 50$ mm. In this figure, the results are shown for shear force acting along the major minor axis.

Table 1. Collapse pressure for elliptic cylinders under external pressure, $a = 101.6\,\text{mm}$, $b = 50.8\,\text{mm}$, $E = 3241.4\,\text{MPa}$, and $\nu = 0.37$. Note: (1) – Yao and Jenkins (1970); (2) – Marlowe and Brogan (1971), (3) – Bushnell (1971)

Thick-ness [mm]	Length [mm]	Collapse pressure [MPa]				
		(1)		(2)	(3)	ABAQUS
		Experimental				
0.737	101.6	0.006	0.0069	0.0068	0.0076	0.0074
0.77	152.4	0.0046	0.00455	0.0046	0.0051	0.005
0.737	254.0	0.0028	0.0027	0.00276	0.003	0.0032
2.31	254.0	0.031	0.057	0.037	0.04	0.045
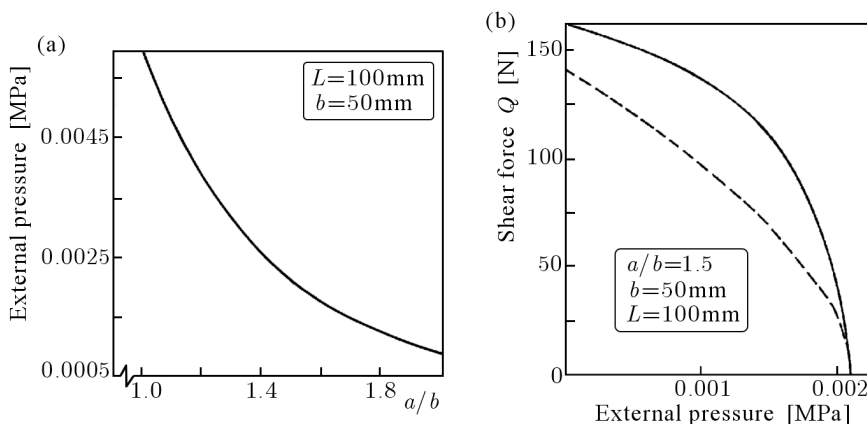
Fig. 14. Effect of the semi-axes ratio a/b on buckling pressure of the elliptic cylinder (a). Combined stability domains for elliptic cylinders when loaded by the horizontal shear force and external pressure (b), - - - shear force along major axis, —— shear force along minor axis

3.   Experimental results

Experiments were carried out on cylinders made of the Mylar sheet. Thickness of the Mylar sheet was measured with the help of a linear Mitutoyo's gauge having an automatic retention of minimum thickness reading between two balls. It was found that thickness of sheet was 0.25 mm. Details concerning model preparation can be found in the work by Błachut and Jaiswal (2008).

Buckling tests were carried out using a rig sketched in Fig. 15. The horizontal force was applied using the push-bar, and the use of partial vacuum

inside of the inner cylinder represented the external pressure. Again, the experimentation details can be found in the work by Błachut and Jaiswal (2008).
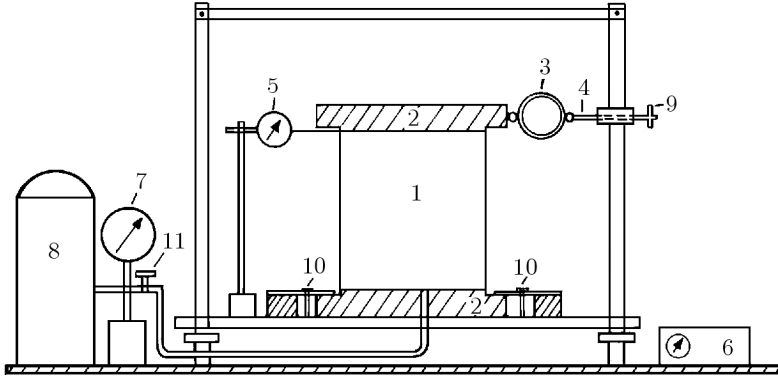
Fig. 15. Test rig for testing Mylar cylinder under the edge shear force and external pressure; 1 – Mylar cylinder, 2 – Aluminium flanges, 3 – Load cell to measure force, 4 – Push bar, 5 – Dial gauge to measure deflection, 6 – B&K strain gauge meter, 7 – Vacuum gauge, 8 – Vacuum chamber, 9 – bolt to apply push, 10 – Clamping bolts

3.1. Circular cylinders under edge shear force and external pressure

Four circular cylinders with $R = 50.26$ mm and $R = 99.85$ mm were tested under the edge shear force. Experimental values of the buckling shear force are given in Table 2. Comparisons of typical load-deflection curves from the experiment and ABAQUS are shown in Fig. 16. It is seen that the experimental results well agree with ABAQUS predictions. It can be mentioned here that in the experiment, the buckling under the edge shear force occurs gradually. At a certain load value, wrinkles start to appear on the surface, and then the shear displacement grows more rapidly with the force. This load value at which the first wrinkle appears on the specimen is taken as the bifurcation force Q_{bif}.

Next four circular cylinders were tested under external pressure. Values of experimental and numerical results are given in Table 3. In this case, the results are in good agreement as well. Under external pressure, the buckling occurred suddenly, and there was no difficulty in identifying the buckling pressure. It is seen in Tables 2 and 3 that after reaching the buckling load, the cylinders were re-tested again. For example, the circular cylinder $R = 50.26$ mm, $L = 50$ mm in Table 2 was tested twice. The tests revelated the buckling shear force of 225.0 N and 230 N, respectively.

Table 2. Comparison of experimental and numerical results for the buckling shear force Q_{bif} in circular cylinders

R [mm]	L [mm]	Q_{bif} [N]	
		Experiment	ABAQUS
50.26	50.0	225.0 230.0	227.5
	100.0	163.7 162.0 171.0 172.4	162.9
	150.0	132.0 139.0	135.5
99.85	100.0	180.0 184.0 186.0 198.0	188.3
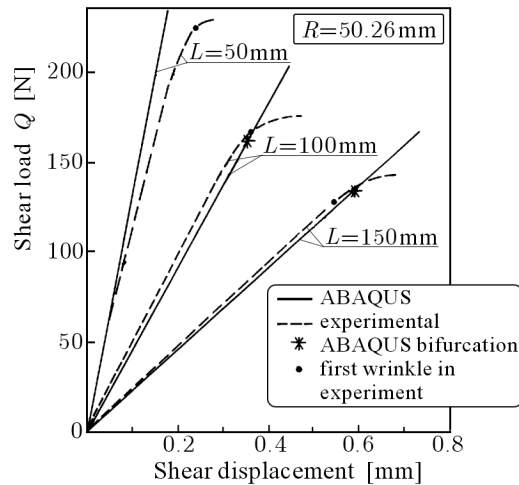
Fig. 16. Comparison of experimental and numerical (ABAQUS) results on the load-deflection curve for the circular cylinder under the edge shear force

The next phase of experiments was devoted to tests under simultaneous action of the external pressure and horizontal edge force. Two pairs of new cylinders were used there, i.e., two specimens each of $R = 50.26$ mm and $R = 99.85$ mm. The results of these tests are given in Tables 4 and 5. A comparison of the experimental results with numerical ones is shown in Fig. 17.

Table 3. Comparison of experimental and numerical results for buckling pressure P_{bif} in the case of circular cylinders. Numbers in brackets indicate the number of circumferential waves.

R [mm]	L [mm]	P_{bif} [MPa]	
		Experiment	ABAQUS
50.26	50.0	0.011 (10)	0.0114 (11)
	100.0	0.00516 (8) 0.0055 (8) 0.0060 (8)	0.0059 (8)
	150.0	0.0036 (6) 0.004 (6)	0.0039 (6)
99.85	100.0	0.002 (12) 0.002 (12)	0.002 (14)

Table 4. Experimental results on buckling of circular cylinders under a combined loading of the edge shear force and external pressure; $R = 50.26$ mm.

Specimen No. 1		Specimen No. 2	
Q [N]	P_{bif} [MPa]	Q [N]	P_{bif} [MPa]
0.0	0.0055	0.0	0.006
30.0	0.0055	30.0	0.006
60.0	0.0055	60.0	0.0058
90.0	0.0045	90.0	0.005
121.5	0.004	120.0	0.004
135.0	0.003	150.0	0.002
150.0	0.002	165.0	0.001
157.5	0.0015	173.7	0.0
171.0	0.0	–	–

3.2. Concentric circular cylinders under edge shear force

Concentric cylinders required a special set of aluminium flanges to be used at the top-end of the models, see Błachut and Jaiswal (2008) for details. Three, nominally identical, concentric cylinders were manufactured and tested under the edge horizontal shear force. The experimental results obtained are given in Table 6. The load deflection curve for one such a test is shown in Fig. 18. It is seen that although the experimental load-deflection curve for concentric cylinders shows some decrease in stiffness, it does not well agree with numerical prediction of the critical shear force Q_{bif}. In fact, the experimental buckling

Table 5. Experimental results on buckling of circular cylinders under a combined loading of the edge shear force and external pressure; $R = 99.85$ mm.

Specimen No. 1		Specimen No. 2	
Q [N]	P_{bif} [MPa]	Q [N]	P_{bif} [MPa]
0.0	0.002	0.0	0.002
30.0	0.0019	30.0	0.00175
60.0	0.0017	60.0	0.00175
90.0	0.0016	90.3	0.0015
120.0	0.0012	136.2	0.00125
154.0	0.00075	152.4	0.001
188.0	0.0	186.0	0.0
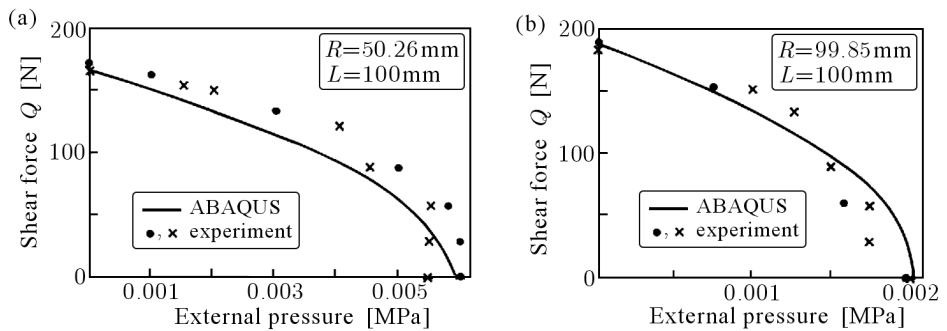
Fig. 17. Comparison of experimental and numerical, ABAQUS, results for circular cylinder under combined loading of edge shear force and external pressure

Table 6. Comparison of experimental and numerical results for concentric cylinders under the edge shear force, $R_1 = 100.145$ mm, $R_2 = 50.215$ mm, $L_1 = L_2 = 100$ mm. Note: for the case *, the load-deflection is shown in Fig. 18

Q_{bif} [N]	
Experimental	ABAQUS
210.0	
217.5*	267.7
170.0	

force is always less than the numerical results. It is felt that this could be due to pre-stressing induced in the inner cylinder while mounting the top flange.
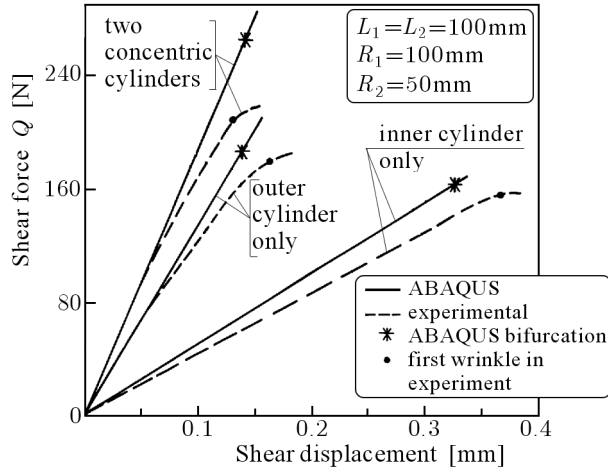
Fig. 18. Comparison of experimental and numerical (ABAQUS) results on the
load-deflection curve for concentric cylinders under the edge shear force

3.3. Elliptic cylinders under edge shear force and external pressure

Next, six elliptic cylinders were tested for buckling under the action of a horizontal shear force. Geometry of these shells is given in Table 7. Each shell was loaded up to buckling level, then unloaded, and then tested again. This gave twelve values of the buckling shear force Q_{bif}. Comparison of experimental and numerical results on the buckling shear force is given in Table 7. In Figs. 19 and 20, the comparison between the experimental and numerical load deflection curves is depicted for various a/b ratios. It is seen that the experimental results well agree with numerical predictions.

Table 7. Comparison of experimental and numerical results on the buckling shear force for elliptic cylinders, $L = 100$ mm

b [mm]	a [mm]	a/b	Shear force Q_{bif} [N] along			
			major axis		minor axis	
			Experiment	ABAQUS	Experiment	ABAQUS
50.035	55.05	1.1	162.0 169.5	158.7	177.0 180.0	168.5
50.035	65.01	1.299	150.0 165.0	149.1	169.5 174.3	171.3
50.035	75.00	1.499	139.5 147.0	140.3	171.0 170.0	162.2
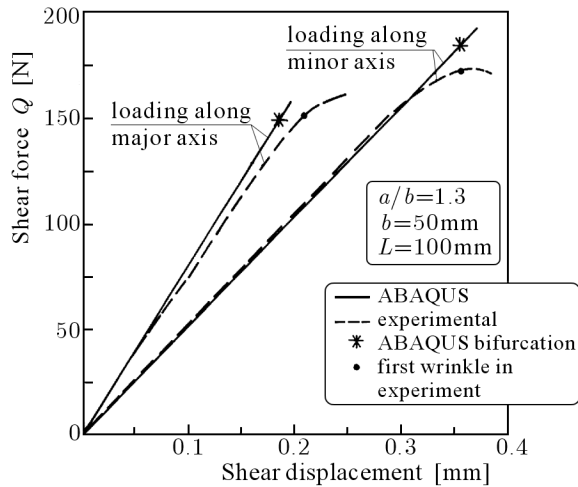
Fig. 19. Comparison of experimental and numerical (ABAQUS) results on the load-deflection curve under the edge shear force for the elliptic cylinder, $a/b = 1.3$
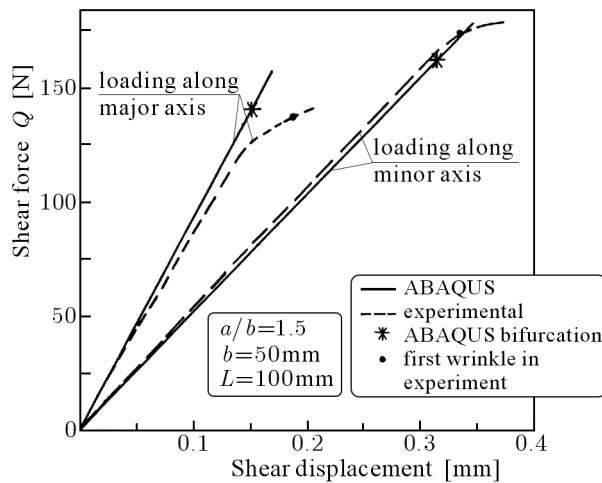
Fig. 20. Comparison of experimental and numerical (ABAQUS) results on load-deflection curves for the edge shear force applied to the elliptic cylinder, $a/b = 1.5$

In the subsequent phase of tests, the same elliptic models were used to investigate the buckling resistance against external pressure. The experimental results on buckling pressure are given in Table 8 along with numerical predictions. It is seen that these results well agree with numerical predictions by FE analyses. In the case of elliptic cylinders, the buckling under external pressure

occurs suddenly as well, and there is no difficulty in identifying the buckling pressure. Moreover, unlike in circular cylinders, there are no uniform circular waves in this case.

Table 8. Comparison of experimental and numerical results on the buckling pressure for elliptic cylinders, $L = 100\,\text{mm}$

b	a	a/b	P_{bif} [MPa]	
			Experiment	ABAQUS
50.035	55.05	1.1	0.005 0.0045 0.00475	0.00494
50.035	65.01	1.299	0.003 0.00325 0.00325	0.00316
50.035	75.00	1.499	0.0021 0.00225 0.00225	0.00209

4. Conclusions and closure

Numerical results on buckling of concentric cylinders under the edge shear force indicate that the critical shear displacement δ_c plays an important role in deciding about the buckling pattern. For an optimal design, the inner and outer cylinder should have the same δ_c.

Efforts made on the experimental study have met with mixed success. For circular cylinders, the experimental results on the buckling shear force and buckling pressure well agree with the ABAQUS prediction. In the experiment, it was found that under the edge shear force, buckling occurs gradually in form of appearing wrinkles on the cylinder. However, under external pressure, cylinders buckle suddenly. Experimental results on buckling of concentric cylinders under the edge shear force poorly agree with ABAQUS results (Fig. 18 and Table 6). It is felt that this is due to difficulties in making a specimen of concentric cylinders. While fixing the top flange on the outer cylinder, some pre-stressing gets induced in the inner cylinder which may make it weaker under the edge shear, and hence the experimental results are on the lower side. A more detailed experimental study would be well justified here.

The experimental results on elliptic cylinders under the edge shear force show favourable comparison with the ABAQUS predictions (as seen in Figs. 19, 20 and Table 7). During the experiments, the position of vertical joint in the Mylar cylinder was found to have influence on the buckling force. To minimise this influence, the joint should be positioned below the point of force application. Here, like in circular cylinders, the buckling occurs gradually too.

For elliptic cylinders under external pressure, the experimental results well agree with those of ABAQUS (Table 8). Under external pressure, the buckling occurs suddenly and there is no difficulty in identifying the buckling pressure. Under external pressure, all the elliptic cylinders considered in this study, failed suddenly by buckling bifurcation with a number of circumferential lobes. For these cylinders the b/t ratio was 200. In previous studies on elliptic cylinders under external pressure (Yao and Jenkins, 1970; Bushnell, 1971; Marlowe and Brogan, 1971) failure occurred due to collapse. These cylinders were comparatively thick with the maximum $b/t = 68.96$. To evaluate the influence of thickness on the buckling mode of Mylar cylinders, some numerical results on buckling for various values of thickness were obtained. These are given in Table 9. It is seen that thin cylinders indeed fail by buckling bifurcation, and thick ones fail by collapse with transition occurring between $b/t = 150$ and $b/t = 100$.

Table 9. Effect of thickness on buckling of the elliptic cylinder under external pressure $a/b = 1.5$, $b = 50\,\mathrm{mm}$, $L = 100\,\mathrm{mm}$, $E = 5028.5\,\mathrm{MPa}$, $\nu = 0.3$

t [mm]	b/t	Buckling pressure [MPa]	Mode of failure
0.1	500	0.00021	bifurcation
0.167	300	0.00076	bifurcation
0.25	200	0.002	bifurcation
0.333	150	0.00426	bifurcation
0.5	100	0.0113	collapse
1.0	50	–	collapse

References

1. Athiannan K., Palaninathan R., 2004, Buckling of cylindrical shells under transverse shear, *Thin-Walled Structures*, **42**, 1307-1328

2. Błachut J., Jaiswal O.R., 2008, Numerical and experimental study into behaviour of cylinders under edge shear force and external pressure, In: *Proc. of The Ninth Intl Conf. on Computational Structures Technology*, B.H.V. Topping (Edit.), Athens, Greece

3. Błachut J., Magnucki K., 2008, Strength, stability and optimization of pressure vessels – review of selected problems, *Applied Mechanics Reviews, Transactions of the ASME* (in print)

4. Bushnell D., 1971, Stress, buckling and vibration of prismatic shells, *AIAA J.*, **9**, 10, 2004-2013

5. Galletly G.D., Błachut J., 1985, Plastic buckling of short vertical cylindrical shells subjected to horizontal edge shear loads, *J. of Pressure Vessel Technology, Transactions of the ASME*, **107**, 101-106

6. Gettel M., Schneider W., 2007, Buckling strength of cantilevered cylindrical shells subjected to transverse load using Eurocode 3, *J. Constructional Steel Res.*, **63**, 1467-1478

7. Hibbitt, Karlsson and Sorensen Inc., 2004, *ABAQUS standard user's manual*, Version 6.4, Pawtucket, Providence, RI 02860-4847, USA

8. Lu S.Y., 1965, Buckling of cantilever cylindrical shell with a transverse end load, *AIAA J.*, **3**, 2350-2351

9. Marlowe M.B., Brogan F.A., 1971, Collapse of elliptic cylinders under uniform external pressure, *AIAA J.*, **9**, 11, 2264-2266

10. Öry H., Reimerdes H.-G., Gómes Garcia J., 1998, The design of shells and tanks in the aerospace industry: some practical aspects, *Progress in Structural Eng. and Materials*, **1**, 4, 404-414

11. Rotter J.M., 1998, Metal silos, *Progress in Structural Eng. and Materials*, **1**, 4, 428-435

12. Schroeder P., 1972, Über die Stabilität der Querkraftbelasteten dünnwandigen Kreiszylinderschale, *ZAMM*, **52**, T145-T148

13. Singer J., Arbocz J., Weller T., 2002, *Buckling Experiments: Experimental Methods in Buckling of Thin-Walled Structures*, John Wiley & Sons Inc., New York

14. Yamaki N., 1984, *Elastic Stability of Circular Cylindrical Shells*, North-Holland series in Applied Mathematics and Mechanics, Amsterdam

15. Yao J.C., Jenkins W.C., 1970, Buckling of elliptic cylinders under normal pressure, *AIAA J.*, **8**, 1, 22-27

Sprężyste wyboczenie powłoki walcowej poprzeczną siłą ścinającą

Streszczenie

Praca przedstawia wyniki obliczeń numerycznych oraz wyniki doświadczalne dotyczące sprężystego wyboczenia powłok walcowych poddanych: (i) działaniu ciśnienia zewnętrznego, (ii) działaniu skupionej siły poprzecznej przyłożonej do końca powłoki, (iii) równoczesnym działaniu obydwu obciążeń. Przedmiotem pracy są natępujące trzy konfiguracje geometryczne: (i) pojedyncza pionowa powłoka walcowa, (ii) układ dwóch pionowych i współosiowych powłok walcowych, (iii) pionowa powłoka walcowa o przekroju eliptycznym. Testy wykonano na 19 powłokach. Otrzymane wyniki doświadczalne porównano z wynikami obliczeń numerycznych. Dobrą zgodność wyników doświadczalnych i teoretycznych otrzymano w przypadku wszystkich konfiguracji z wyjątkiem powłok współosiowych.

Praca analizuje zachowanie się pionowych powłok walcowych w warunkach utraty stateczności, a w przypadku powłok współosiowych zajmuje się interakcją pomiędzy wewnętrznym i zewnętrzym walcem. Podano szczegółową analizę wzajemnej interakcji tych powłok.